Bacterial protein interaction networks: connectivity is ruled by gene conservation, essentiality and function

Maddalena Dilucca,[1] Giulio Cimini,[2, 3] and Andrea Giansanti[1, 4]

[1] *Physics Department, Sapienza University of Rome, 00185 Rome (Italy)*
[2] *Physics Department and INFN, University of Rome Tor Vergata, 00133 Rome (Italy)*
[3] *Institute for Complex Systems (CNR) UoS Sapienza, 00185 Rome (Italy)*
[4] *INFN Roma1 unit, Sapienza University of Rome, 00185 Rome (Italy)*

Protein-protein interaction (PPI) networks are the backbone of all processes in living cells. In this work we relate conservation, essentiality and functional repertoire of a gene to the connectivity k (i.e., the number of interaction links) of the corresponding protein in the PPI network. On a set of 42 bacterial genomes of different sizes, and with reasonably separated evolutionary trajectories, we investigate three issues: i) whether the distribution of connectivities changes between PPI subnetworks of essential and nonessential genes; ii) how gene conservation, measured both by the evolutionary retention index (ERI) and by evolutionary pressures, is related to the the connectivity of the corresponding protein; iii) how PPI connectivities are modulated by evolutionary and functional relationships, as represented by the Clusters of Orthologous Genes (COGs). We show that conservation, essentiality and functional specialisation of genes constrain the connectivity of the corresponding proteins in bacterial PPI networks. In particular, we isolate a core of highly connected proteins (with connectivities $k \geq 40$), which is ubiquitous among the species considered here – though mostly visible in the degree distributions of bacteria with small genomes (less than 1000 genes). The genes that belong to this highly connected core are conserved, essential and, in most cases, belong to the COG cluster J, related to ribosomal functions and to the processing of genetic information.

Keywords: Protein-protein interactions, Gene Essentiality, Evolutionary Retention Index, Clusters of Orthologous Genes

I. INTRODUCTION

To operate biological activities in living cells, proteins work in association with other proteins, often assembled in large complexes. Hence, knowing the interactions of a protein is important to understand its cellular functions. Moreover, a comprehensive description of the stable and transient protein-protein interactions (PPIs) within a cell would facilitate the functional annotation of all gene products, and provide insight into the higher-order organisation of the proteome [1, 2]. Several methodologies have been developed to detect PPIs, and have been adapted to chart interactions at the proteome-wide scale. These methods, combining different technologies, experiments and computational analyses, generate PPI networks of sufficient reliability, enabling the assignment of several proteins to functional categories [3, 4]. Moreover, the statistical study of bacterial PPIs over several species (meta-interactomes) has brought important knowledge about protein functions and cellular processes [5, 6].

Our aim here is to shed some light on the relationships among conservation, essentiality and functional annotation at the genetic level and connectivities of PPI networks, at the protein level. We extend here our previous observations made on the PPI of *E.coli* which suggested a strong correlation between the connectivity of PPI networks on the one hand, and codon bias, gene conservation and essentiality on the other hand [7, 8]. It is worth, in the next two paragraphs, specifying what is usually meant by gene essentiality and gene conservation.

Individual genes in the genome contribute differently to the survival of an organism. According to their known functional profiles and based on experimental evidence, genes can be divided into two categories: essential, and nonessential ones [9, 10]. Essential genes are not dispensable for the survival of an organism in the environment it lives in [10, 11]. Nonessential genes are instead those which are dispensable [12], being related to functions that can be silenced without compromising the survival of the organism. Naturally, each species has adapted to one or more evolving environments and, plausibly, genes that are essential for one species may be not essential for another one.

It has been argued many times that essential genes are more conserved than nonessential ones [13–17]. The term ”conservation” has, however, at least two meanings. On the one hand, a gene is conserved if orthologous copies of it are found in the genomes of many species, as measured by the Evolutionary Retention Index (ERI) [9, 18]. On the other hand, a gene is (evolutionarily) conserved when it is subject to a purifying, selective, evolutionary pressure, which disfavours mutations. A common measure of evolutionary pressure is K_a/K_s, the ratio of the number of non synonymous substitutions per non synonymous site to the number of synonymous substitutions per synonymous site. In this second meaning a conserved gene is, in a nutshell, a slowly evolving gene, a gene that hardly incorporates mutations [13, 19]. To measure the evolutionary pressures exerted on the genes we use here K_a/K_s, and to measure evolutionary patterns of codon bias we use the Effective Number of Codons (ENC) plots.

The main finding of this work is the presence, in bacterial PPI networks, of a functional transition ruled by the connectivity (degree k) of proteins. The genes of proteins with high connectivities are under selective pressure, conserved, and essential. Below the transition ($k < 50$), the functional repertoire of low connectivity proteins is heterogeneous, whereas the genes of proteins with $k > 50$ mainly belong to the Cluster of Orthologous Genes (COG) J (related to translation, ribosomal structure and biogenesis), with just a few interesting hubs belonging to COGs I (Lipid transport and metabolism), K (Transcription) and L (Replication, recombination and repair). Moreover, we show that in the degree distribution of each bacterial PPI network there is an ubiquitous trace of an almost-invariant structure of conserved hubs, essentially due to the ribosomal protein complexes, mostly visible in the networks of bacteria with small genomes.

MATERIALS AND METHODS

Bacterial dataset and PPI networks

We consider a set of 42 bacterial genomes (that we have previously investigated in [8]), here collected in Table I. Nucleotide sequences were downloaded from the FTP server of the National Center for Biotechnology Information [20]. These genomes were chosen in order to have a reasonably large coverage of data concerning conservation, essentiality and selective pressure.

PPIs are obtained from the STRING database (Known and Predicted Protein-Protein Interactions, `https://string-db.org/`)[21]. We have chosen STRING because of its quite large coverage of different bacterial species, useful to extend to multiple species the study we did in [7]. In STRING, each interaction is assigned with a confidence level or probability w, evaluated by comparing predictions obtained by different techniques [22–24] with a set of reference associations, namely the functional groups of KEGG (Kyoto Encyclopedia of Genes and Genomes) [25]. In this way, interactions with high w are likely to be true positives, whereas, a low w possibly corresponds to a false positive. As usually done in the literature, we consider only interactions with $w \geq 0.9$, a threshold that provides a fair balance between coverage and interaction reliability (see for instance the case study on *E.coli* reported in [7]). We denote by k the *degree* (number of connections) associated to each protein in each PPI network after the thresholding procedure. Note also that after applying the cut-off we are left, for each network, with a number of isolated proteins (singletons, with no connections) that grows as $\sqrt{n}$ (where n is the number of proteins in the genome). These isolated proteins are not considered in the network analysis and are regarded as stemming from statistical noise or just appear isolated because the PPI data is incomplete.

It is known that PPIs of some species in our dataset might be known much better than others (this is for instance the case of *E.Coli*). To investigate potential bias in the dataset, we checked that the densities of PPIs are high for small genomes and tend to be constant and not so different from that of *E.coli* in bacteria with bigger genomes (see bottom panel of Figure S7). Moreover, the big genomes in our dataset include highly investigated pathogens.

The distinction between small and big genomes is a key emergent point in this work. We divide the set of 42 bacterial genomes in three groups, according to the number n of their genes: a) $n < 1000$, b) $1000 < n < 3000$ and c) $n > 3000$. In the Supplementary Information we have addressed the dependence of various network properties on the size of the genome.

Gene Conservation: ERI and $\mathbf{K_a/K_s}$

The Evolutionary Retention Index (ERI) [9] is a way of measuring the degree of conservation of a gene. In the present study the ERI of a gene is the fraction of genomes, among those reported in Table I, that have at least an orthologous (same COG label) of the given gene. Then, as reminded in the Introduction, a low ERI value is related to a gene which is rather specific, common to a small number of genomes; whereas high ERI is characteristic of highly shared, putatively universal and essential genes.

We also consider another notion of gene conservation. Conserved genes are those which are subject to a purifying, conservative evolutionary pressure. To discriminate between genes subject to purifying selection and genes subject to positive selective Darwinian evolution, we use a classic but still widely used indicator, the ratio K_a/K_s between the number of non synonymous substitutions per non synonymous site (K_a) and the number of synonymous substitutions per synonymous site (K_s) [19]. This parameter represents a straightforward and effective way of separating genes subject to purifying evolutionary selection ($K_a/K_s < 1$) from genes subject to positive selective Darwinian evolution ($K_a/K_s > 1$). There are different methods to evaluate this ratio, though the alternative approaches are quite consistent among themselves. For the sake of comparison, we have used here the K_a/K_s estimates by Luo et al. [15] that are based on the Nej and Gojobori method [26]. Note that each genome has a specific average level of K_a/K_s [7].

Gene Essentiality

We used the Database of Essential Genes (DEG, `www.essentialgene.org`) [15], which classifies a gene as either essential or nonessential, on the basis of a combination of experimental evidence (null mutations or transposons) and general functional considerations. DEG collects genomes from Bacteria, Archaea and Eukarya, with different degrees of coverage[27, 28]. Of the 42 bacterial genomes we consider, only 23 are covered—in toto or partially—by DEG, as indicated in Table I.

ENC plot

The ENC-plot is a well known tool to investigate the patterns of synonymous codon usage in which the ENC (Effective Number of Codons) values are plotted against GC_3 (Guanine and Cytosine Content at the third codon position). The formula of ENC values expected under the hypothesis of pure mutational bias (no selection) is given by:

$$ENC = 2 + s + \frac{29}{s^2 + (1-s)^2} \tag{1}$$

where s represents the value of GC_3 [29]. When the corresponding points fall near the expected neutral curve, mutations that enforce the typical mutational bias of the species are the main factor affecting the observed codon diversity. Whereas when the corresponding points fall considerably below the expected curve, the observed codon usage bias of the species is mainly affected by natural selection. To quantitatively represent the balance between mutational bias and selective natural pressure we parametrise the ENC formula, to be used in non-linear fits to the experimental data:

$$ENC = a + b * s + \frac{c}{s^2 + d * (1-s)^2}. \tag{2}$$

ENC plots of genes corresponding to low, intermediate and high connectivity proteins are shown in Figure S9. The best fit parameters for the three groups of genes are collected in Table VI.

Clusters of orthologous proteins

We use the functional annotation given in the database of orthologous groups of proteins (COGs) from Koonin's group, available at `http://ncbi.nlm.nih.gov/COG/` [30, 31]. We consider 15 functional COG categories (see Table II), excluding the generic categories R and S for which functional annotation is either too general or missing.

RESULTS AND DISCUSSION

Degree distribution of PPI networks. We start by studying the degree distributions $P(k)$ observed in bacterial PPIs. We first recall that such a distribution was found to be scale-free in *E.coli* [7, 32–34], meaning that the corresponding PPI network features a large number of poorly connected proteins, and a relatively small number of highly connected hubs. In order to assess the generality of this observation, we compute $P(k)$ for each genome in Table I (plots are reported in Figures S10 and S11). Note that, despite the fact that PPI networks of different bacteria have different sizes and densities, their average connectivity and the support of their $P(k)$ are very similar. Thus, we can superpose all the considered bacterial degree distributions without the need to normalise the support of each $P(k)$. When doing so, we observe two distinct regimes (see Figure 1). For low values of $k < 40$, the distribution is approximately scale-free: $P(k) \propto k^{-\gamma}$ ($\gamma = 2.48$). This scaling behaviour is consistent with previous studies on the genomes of yeast, worms and flies [35] and on co-conserved PPIs in some bacteria [36]. The scale free natura of bacterial PPI's is still a matter of debate, and a rough discussion of the origin of this feature is out of the scope of this paper. In this work we generally confirm that, as said above, there is as expected, a large number of poorly connected proteins and a small number of hubs.

Remarkably, for higher values of k the distribution deviates from a power law, and a bump with a Gaussian-like shape emerges. This feature, visible for $k \geq 40$ may be due to the contribution of proteins belonging to large complexes [37]. From the whole set of observation presented in this paper, the bump in the $P(k)$ is due to the complex of ribosomal interactions. Indeed, if one recalculates the degree distribution of a dataset in which the ribosomal proteins are removed the bump is not present (see Figure 1, empty dots). Moreover, if we consider the separate contribution of essential and nonessential genes to the $P(k)$ (for DEG-annotated genomes), we see that the bump is present only in the degree distribution of essential genes. Note also that the degree distributions for essential and nonessential genes are well separated and the average degree is systematically higher for essential genes than for nonessential ones, consistently with previous findings [35]. Remarkably, we have shown in a previous paper [8] that the number of essential genes in bacteria is close to 500 and does not depend on the size of the genome. To correctly interpret the emergence of the bump in the average $P(k)$ in Figure 1 it is worth to point out the distinction between small and not so small genomes. In the small genomes almost all the genes are essential and among the essential genes those belonging to COG J (functions related to translation and ribosomal structure and biogenesis) play a major and ubiquitous role. In Figure S8 we have checked that the bump that emerges in Figure 1 as a feature of essential and conserved genes, is quite visible in the $P(k)$ of small genomes, whereas seems to be confused in the case of bigger genomes. This might be interpreted as a dilution effect; in the networks of bigger genomes there are a lot of specific interactions besides the essential ones. Nevertheless, averaging $P(k)$ over small, intermediate and big genomes we still see the bump and interpret it as an emerging feature due to a core of highly connected proteins (connectivities $k \geq 40$). From these considerations we can exclude that this bump, observed here for

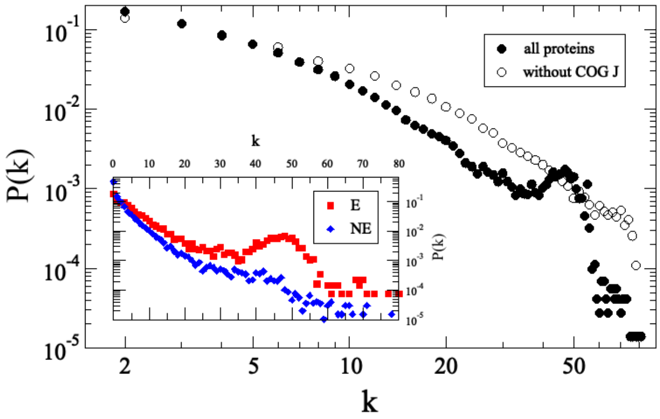

FIG. 1. Probability distribution $P(k)$ for the number of connections k of each protein, averaged over the bacterial species considered in Table I (full dots), compared with the degree distribution after removal of the proteins corresponding to genes in COG J, related to translational processes (empty dots). Inset: $P(k)$ for essential (E) and nonessential (NE) genes, averaged over DEG-annotated genomes. Note that the average degree is higher for essential genes than for nonessential ones, and the two probability distributions are quite distinct. The region of the curve for low k can be well approximated by a power law [38].

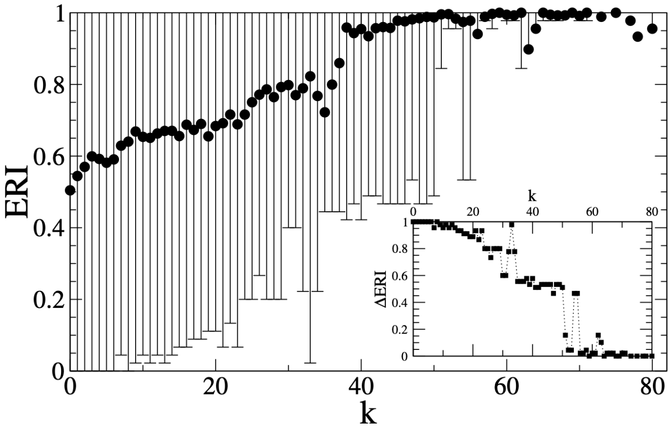

FIG. 2. Average ERI values of bacterial genes as a function of the degrees k of the corresponding proteins, for all the considered genomes. Error bars are standard deviations of ERI values associated to a given k value. Inset: amplitude of the error bar (ΔERI) as a function of k.

the first time, might emerge just because that part of the PPI is much more investigated than other subnetworks: the bump is there because of the ribosome, and this happens for all bacteria.

PPI connectivity and gene conservation We now investigate whether the connectivity k of a protein in a PPI network drives a transition in the degree of conservation (as measured by ERI) of the corresponding genes. Figure 2 displays the average value and the spread of ERI in genes relative to proteins with the same degree in the PPIs of different species. As a general feature we observe that, on the average, the genes of highly connected proteins are highly conserved among the bacterial species we consider, that constitute a reasonably wide sample of different evolutionary adaptations. The same Figure 2 shows that if $k \leq 50$ then the ERI highly fluctuates between different samples of proteins with the same k, in different species. For high connectivities (above $k = 50$), the ERI is close to 1, with a drastic drop in the fluctuation (as shown in the inset). This observation points to the existence, in each bacterial PPI, of an almost-invariant structure of conserved hubs, sustained by highly conserved genes. We can conclude, as a rule of thumb, that a protein with connectivity degree of 40 or more is likely to be coded by a gene shared by at least 80% of the species in a generic pool of bacteria. At the moment, we have not a general explanation for this apparent threshold. Let us just propose, as an heuristic observation, the existence of an almost-critical value of connectivity to be set between 40 and 50, that corresponds to the connectivity of the core of proteins specifically involved, as we have alluded to in the previous paragraph, to the ubiquitous ribosomal functions (see also Tables IV and V).

Evolutionary pressure and PPI connectivity We then look at the evolutionary pressure exerted on genes whose proteins have different connectivities. Figure 3 shows the ratio K_a/K_s for groups of genes binned by the connectivity k of the corresponding proteins, for all the 42 bacterial species in Table I. As is well known this ratio K_a/K_s provides a straightforward indication of the balance between a positive driving *darwinian selection* (when the numerator prevails) and a *purifying*, stabilising selection (acting against change in genes for which the denominator prevails).

We see that the more connected proteins correspond to genes which are subject to an increasing purifying evolutionary pressure. Indeed, the ratio (K_a/K_s) is less than 1 in all bins of connectivity and systematically decreases, as a function of k. A decreasing ratio generally indicates an increasing role of purifying, conservative, darwinian, evolutionary pressure on the corresponding set of genes. This is a reasonable results, pointing out that the groups of genes that support conserved structures of connectivity in the PPIs are more constrained, in evolution, than the genes of less interacting proteins.

To add evidence to this observation we have also considered ENC plots for sets of genes binned by the connectivities of the corresponding proteins. Interestingly, the ENC data in Figure S9 are fully consistent with those in Figure 3. In the ENC plots, the points associated to low connectivity proteins (red) are closer to the so called Wright's profile (represented there as black solid lines) than those associated to proteins with intermediate and high connectivities (green and blue lines). Figure 4 stresses this observation in a more quantitative way by showing that in the ENC plots the average distance from Wright's profile monotonously increases with k, Overall, the above results clearly indicate that codon bias and

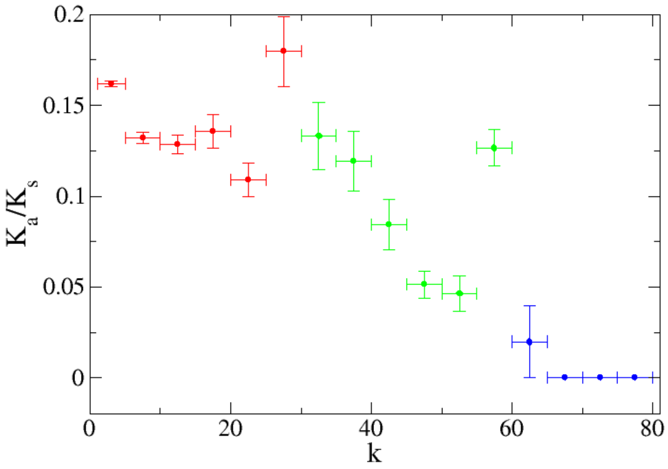

FIG. 3. (K_a/K_s) of groups of genes corresponding to proteins with different connectivity degrees k. As in the following Figures 4 and S9, low connectivities are shown in red, intermediate in green and high connectivities in blue.

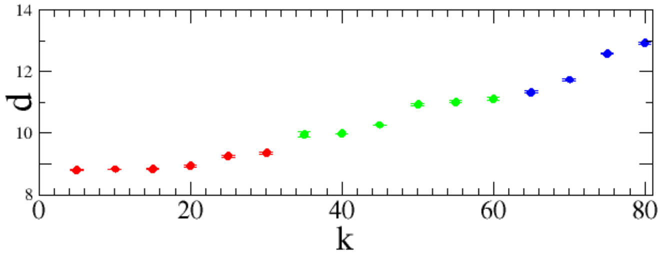

FIG. 4. ENC plot and connectivity. Each point in this graph represents a group of genes, characterised by the average connectivity k of the corresponding proteins in the PPI network and by the average euclidean distance d, in the ENC plot, from Wright's theoretical curve. Different groups of genes are represented with different colors as a function of k. . The distance from the curve clearly increases with k. Wright's curve corresponds, in the ENC plot, to pure mutational bias (see equation (1)), then higher connectivities of the proteins imply bigger evolutionary selective pressure on the corresponding group of genes.

GC content of high connectivity genes are more under selective darwinian pressure than genes coding for low-connectivity proteins, in which the rate of accepted mutations is mainly ruled by neutral mutational bias. These observations point out that the almost-invariant structure of protein hubs we alluded to in the previous paragraph, is supported by and underlying set of genes which are under strong mutational control. Perhaps this is an expected result, but we clearly show it here as a general feature associated to ribosomal ubiquitous and conserved functions.

PPI and Essentiality. To further investigate the relationship between gene essentiality and protein connectivities, we consider DEG-annotated genomes and classify interactions between proteins (links) making reference to the essentiality of the corresponding genes. We distinguish three sets of links: ee (linking proteins from two essential genes), $\bar{e}\bar{e}$ (from two nonessential genes) and $e\bar{e}$ (from an essential gene and a nonessential one). We then compute the *density* of these sets of links respectively as:

$$\rho_{ee} = \frac{|ee|}{\frac{1}{2}E(E-1)}, \tag{3}$$

$$\rho_{\bar{e}\bar{e}} = \frac{|\bar{e}\bar{e}|}{\frac{1}{2}NE(NE-1)}, \tag{4}$$

$$\rho_{e\bar{e}} = \frac{|e\bar{e}|}{\frac{1}{2}E \cdot NE}, \tag{5}$$

where E and NE denote the number of essential and nonessential genes, respectively (self-connections are excluded in our analysis). The denominator is the maximum possible value of the numerator, corresponding to the fully-connected graph. Such densities are then compared with the overall density of the network—restricted to genes classified as either essential or nonessential:

$$\langle \rho \rangle = \frac{|ee| + |\bar{e}\bar{e}| + |e\bar{e}|}{\frac{1}{2}(E+NE)(E+NE-1)}. \tag{6}$$

We use the ratios $r_{ee} = \rho_{ee}/\langle \rho \rangle$, $r_{\bar{e}\bar{e}} = \rho_{\bar{e}\bar{e}}/\langle \rho \rangle$ and $r_{e\bar{e}} = \rho_{e\bar{e}}/\langle \rho \rangle$ to assess the level of connectivity of the subnetworks with respect to the overall connectivity. Table III shows that subnetworks of essential genes are far denser than the overall networks, and that, in general, essential and nonessential genes tend to form network components that are weakly interconnected. This happens because many essential genes encode for ribosomal proteins, which in turn are localised in the ribosomal complex where they have a high probability to interact [39] (see also Table 3 of [8], which shows approximately 25% of essential genes fall into COG J).

Figures S12 and S13 display the superposed adjacency matrices of the ee (red dots), $e\bar{e}$ (violet dots) and $\bar{e}\bar{e}$ (blue dots) subnetworks, thus showing the network features for each individual species. These graphs confirm the dominance of the interactions between the proteins of essential genes (red dots) in the small genomes. The adjacency matrices of bacteria with intermediate and big genomes are dominated by interactions involving proteins supported by non essential genes (blue dots).

PPI connectivity and functional specialisation. For each PPI network, we define the conditional probability that a protein with degree k belongs to a given COG as:

$$P(\text{COG}|k) = P(k|\text{COG})P(\text{COG})/P(k), \tag{7}$$

where $P(k)$ is the degree distribution in the PPI network, $P(\text{COG})$ is the frequency of that COG in the proteome, and $P(k|\text{COG})$ is the degree distribution restricted to that COGs. Figure 5 shows the COG spectrum as a function of k over all the bacteria here considered. Interestingly, we again note a marked transition. Below $k \simeq 40$ the COG spectrum is quite heterogeneous: genes corresponding to proteins with low connectivity are spread over several COGs which correspond to different functions (see Table II). Instead, proteins with more than 40 interactions are likely to be coded by genes belonging to COG J. There are yet a handful of outliers, hubs with connectivities between 57 and 62, that belong to COG I (related to lipid transport and metabolism) and K and L (which, together with J, define the functional class of information storage and processing). The list of these outliers is reported in Table IV. Interestingly, they correspond to RNA polymerases and to enzymes involved in the acetate metabolism. But, which are the genes of COG J that drive the transition?

In Figure 6 we are able to show which genes are the main characters in the transition. We investigate the connectivities of the highly conserved genes (ERI=1, shared by all the species in Table I) belonging to COG J, and whose proteins have connectivities bigger than 40. These highly shared genes corresponding to cores of highly connected ribosomal proteins are listed in Table V. In the heat map of Figure 6 we sort each gene in the COG J in order of descending degree, species by species, and we see that there is a core of genes (in red, lower left sector) that correspond to highly connected proteins, which are also highly shared (ERI = 1, see Table V) among all the species we considered. It is quite clear from this heat mapthat the 42 species in this study can be split into at least two groups (see the cladogram on the left). In the bottom group there is a shared set of genes (the red band at the bottom-left side of the heat map) corresponding to a common core of highly connected ribosomal proteins. This remarkable observation suggests that the species in this group (namely, Synechocystis sp. PCC 6803, Escherichia Coli K-12 MG1655, Clostridium acetobutylicum ATCC 824, Mycobacterium tuberculosis H37Rv, Sphingomonas wittichii RW1, Vibrio cholerae N16961, Burkholderia thailandensis E264, Rickettsia prowazekii str. Madrid E, Agrobacterium tumefaciens (fabrum), Ralstonia solanacearum GMI1000, Xylella fastidiosa 9a5c) should have a common structural and functional organisation of their ribosomes − An Interesting point to be further investigated. In the rest of the species the connectivity of the proteins, corresponding to the highly shared COG J genes, with $k > 40$ is more heterogeneous. We can conclude that the abrupt transition shown in Figure 5 is driven by a subset of COG J genes which are highly conserved among a subset of species and are listed in Table V. As one can see these genes correspond to a specific subset of ribosomal proteins in the small and large subunits that should be further investigated in their functional and structural role.

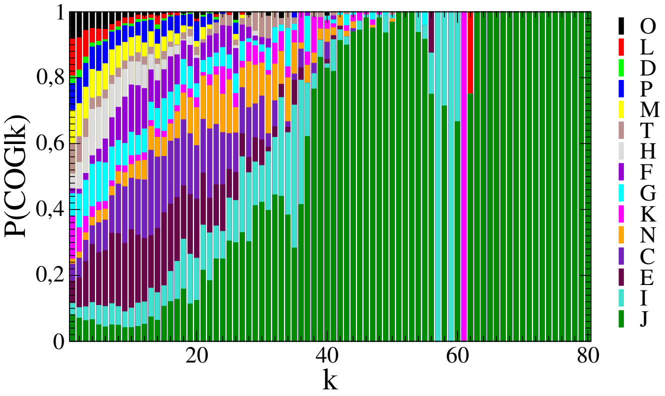

FIG. 5. Probability distribution $P(\text{COG}|k)$ of belonging to a given COG for proteins with degree k, over all considered genomes. Proteins with low connectivity have a very heterogeneous COG composition, whereas, those with high k basically belong only to COG J.

CONCLUSIONS

Connectivity analysis of biological networks, such as protein-protein interaction or metabolic networks, has demonstrated that structural features of network subgraphs are correlated with biological functions [40, 41]. For instance, it was shown that highly connected patterns of proteins in a PPI are fundamental to cell viability [42]. In this work we have shown the existence of a functional transition in bacterial species, ruled by the connectivity of proteins in the PPI networks. The critical threshold in k of the transition is located between $k = 40$ and $k = 50$. Proteins that have connectivities above the threshold are mostly encoded by genes that are conserved, under selective pressure (as measured both by ERI and K_a/K_s) and essential. Moreover the functional repertoire above the threshold focuses mainly on the COG J (Translation, ribosomal structure and biogenesis), with just a few interesting hubs belonging to COGs I (Lipid transport and metabolism), K (Transcription) and L (Replication, recombination and repair).

Indeed, the PPI network of each bacterial species is characterised by a highly connected core of conserved ribosomal proteins, the components of multi-subunit complexes whose corresponding genes are mostly essential [32, 36] and code for supra-molecular complexes, that pile up in the bump we have observed for the degree distribution (Figure 1). Hence, what we are seeing here is essentially the ribosome, and related protein complexes such as RNA Polymerase. Indeed, the ribosome is the only molecular machine in bacteria in which a given protein could legitimately have 40 or more protein binding partners, with the help of rRNA mediating interactions [43].

Admittedly, since there are bacterial species that are much more investigated than others, comparative statistical studies of bacterial PPIs might be particularly biased by the choice of the sample of genomes to be in-

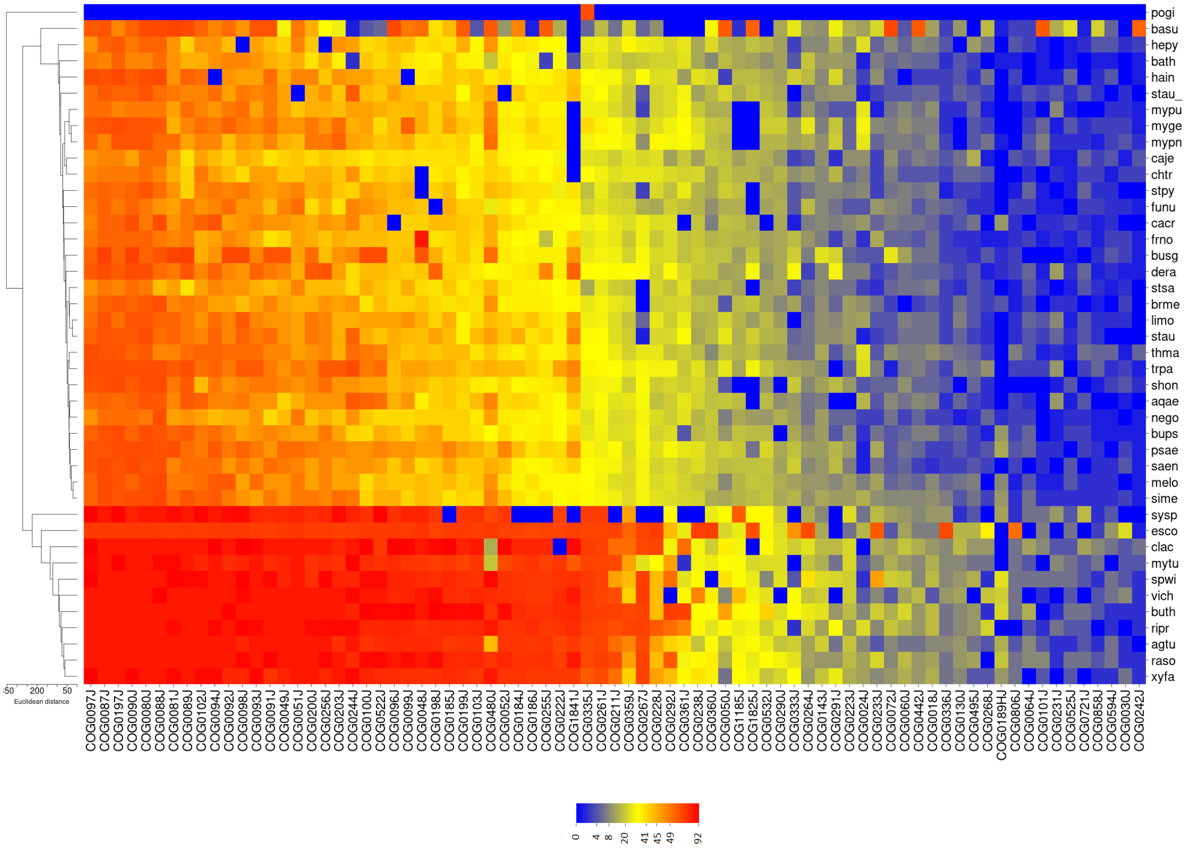

FIG. 6. Heat map of the connectivity degree of the protein as distributed over the COG J genes with ERI=1, in each species. Genes are sorted by decreasing average degree. We note that those genes which correspond to degrees bigger than 40 are conserved for all species. Details of these genes are provided in Table V.

cluded in the study. Our dataset is no exception. In order to assess this possible bias in our study we have checked that in our dataset we have included small genomes (i.e. less than 1000 genes) whose PPIs have densities (a rough proxy for the coverage of the interactions in the network) that are higher than those of bigger genomes (Figure S7). The group of small genomes comprises Buchnera, Chlamydia, Mycoplasmas, whereas bigger genomes refer mostly to illustrious pathogens that are surely among the most investigated bacterial species. The densities of the networks of these species are quite similar and comparable with that of *E.coli*. As a general rule, and quite obviously, the networks relative to small genomes are better covered in the STRING database (after the application of a conservative cutoff $w = 900$) than those relative to bigger genomes. Interestingly, we have shown that, indeed, the PPI adjacency matrices of bacteria with small genomes are dominated by the interactions constituting the ribosomal complex. In the adjacency matrices of the PPIs of bacteria with bigger genomes, the cloud of interactions between the proteins of non essential genes tends to superpose to the ever present ribosomal core. In conclusion, we believe to have convincingly shown that bacterial PPIs are characterised by the presence of a highly connected structure, associated to the ribosomal functions, and particularly visible in bacteria with small genomes.

The observations we have presented here could be useful for the prediction of gene essentiality, based on the knowledge of PPI networks, and for the prediction of interactions between proteins, based on genetic information[44, 45]. It is interesting to note that our results are consistent with a previous study based on inferred bacterial co-conserved networks based on phylogenetic profiles [36]. This work suggests to further and systematically investigate how the structure of the PPI networks is correlated with multiple networks at the genetic level, at least in unicellular organisms. In particular we believe that a recent approach based on the introduction of multiple-layer networks could be of great potential interest (e.g. to search for a general scheme behind antimicrobial resistance [46–50]).

[1] G. Drewes and T. Bouwmeester, Global approaches to protein–protein interactions, Current Opinion in Cell Biology **15**, 199 (2003).

[2] E. Golemis and P. Adams, *Protein-protein Interactions: A Molecular Cloning Manual* (Cold Spring Harbor Laboratory Press, 2005).

[3] C. von Mering, R. Krause, B. Snel, M. Cornell, S. G. Oliver, S. Fields, and P. Bork, Comparative assessment of large-scale data sets of protein-protein interactions, Nature **417**, 399 (2002).

[4] A. H. Y. Tong, B. Drees, G. Nardelli, G. D. Bader, B. Brannetti, L. Castagnoli, M. Evangelista, S. Ferracuti, B. Nelson, S. Paoluzi, M. Quondam, A. Zucconi, C. W. V. Hogue, S. Fields, C. Boone, and G. Cesareni, A combined experimental and computational strategy to define protein interaction networks for peptide recognition modules, Science **295**, 321 (2002).

[5] M. Shatsky, S. Allen, B. L. Gold, N. L. Liu, T. R. Juba, S. A. Reveco, D. A. Elias, R. Prathapam, J. He, W. Yang, E. D. Szakal, H. Liu, M. E. Singer, J. T. Geller, B. R. Lam, A. Saini, V. V. Trotter, S. C. Hall, S. J. Fisher, S. E. Brenner, S. R. Chhabra, T. C. Hazen, J. D. Wall, H. E. Witkowska, M. D. Biggin, J.-M. Chandonia, and G. Butland, Bacterial interactomes: Interacting protein partners share similar function and are validated in independent assays more frequently than previously reported, Mol Cell Proteomics **15**, 1539 (2016).

[6] J. H. Caufield, C. Wimble, S. Shary, S. Wuchty, and P. Uetz, Bacterial protein meta-interactomes predict cross-species interactions and protein function, BMC Bioinformatics **18**, 171 (2017).

[7] M. Dilucca, G. Cimini, A. Semmoloni, A. Deiana, and A. Giansanti, Codon bias patterns of e. coli's interacting proteins, PLoS ONE **10**, e0142127 (2015).

[8] M. Dilucca, G. Cimini, and A. Giansanti, Essentiality, conservation, evolutionary pressure and codon bias in bacterial genomes, Gene **663**, 178 (2018).

[9] S. Gerdes, M. Scholle, J. Campbell, G. Balazsi, E. Ravasz, M. Daugherty, A. Somera, N. Kyrpides, I. Anderson, M. Gelfand, *et al.*, Experimental determination and system level analysis of essential genes in escherichia coli mg1655, Journal of Bacteriology **185**, 5673 (2003).

[10] G. Fang, E. Rocha, and A. Danchin, How essential are nonessential genes?, Molecular Biology and Evolution **22**, 2147 (2005).

[11] C. Peng and F. Gao, Protein localization analysis of essential genes in prokaryotes, Scientific Reports **4**, 6001 (2014).

[12] Y. Lin, F. Gao, and C.-T. Zhang, Functionality of essential genes drives gene strand-bias in bacterial genomes, Biochemical and Biophysical Research Communications **396**, 472 (2010).

[13] L. D. Hurst and N. G. Smith, Do essential genes evolve slowly?, Current Biology **9**, 747 (1999).

[14] I. K. Jordan, I. B. Rogozin, Y. I. Wolf, and E. V. Koonin, Essential genes are more evolutionarily conserved than are nonessential genes in bacteria, Genome Research **12**, 962 (2002).

[15] H. Luo, F. Gao, and Y. Lin, Evolutionary conservation analysis between the essential and nonessential genes in bacterial genomes, Scientific Reports **5**, 13210 (2015).

[16] O. Ish-Am, D. M. Kristensen, and E. Ruppin, Evolutionary conservation of bacterial essential metabolic genes across all bacterial culture media, PLoS ONE **10**, e0123785 (2015).

[17] D. Alvarez-Ponce, B. Sabater-Muñoz, C. Toft, M. X. Ruiz-González, and M. A. Fares, Essentiality is a strong determinant of protein rates of evolution during mutation accumulation experiments in escherichia coli, Genome Biology and Evolution **8**, 2914 (2016).

[18] T. Bergmiller, M. Ackermann, and O. K. Silander, Patterns of evolutionary conservation of essential genes correlate with their compensability, PLoS Genetics **8**, e1002803 (2012).

[19] L. D. Hurst, The K_a/K_s ratio: diagnosing the form of sequence evolution, Trends in Genetics **18**, 486 (2002).

[20] D. A. Benson, M. Cavanaugh, K. Clark, I. Karsch-Mizrachi, D. J. Lipman, J. Ostell, and E. W. Sayers, Genbank, Nucleic Acids Research **41**, D36 (2013).

[21] M. J. Szklarczyk, The string database in 2017: quality-controlled protein–protein association networks, made broadly accessible., Nucleic Acids Research **45**, D362 (2017).

[22] C. T. Chien, P. L. Bartel, R. Sternglanz, and S. Fields, The two-hybrid system: A method to identify and clone genes for proteins that interact with a protein of interest, Proceedings of the National Academy of Science **88**, 9578 (1991).

[23] E. M. Phizicky and S. Fields, Protein-protein interactions: Methods for detection and analysis, Microbiological Reviews **59**, 94 (1995).

[24] O. Puig, F. Caspary, G. Rigaut, B. Rutz, E. Bouveret, E. Bragado-Nilsson, M. Wilm, and B. Séraphin, The tandem affinity purification (tap) method: A general procedure of protein complex purification, Methods **24**, 218 (2001).

[25] M. Kanehisa and S. Goto, Kegg: Kyoto encyclopedia of genes and genomes, Nucleic Acids Research **28**, 27 (2000).

[26] M. Nei and T. Gojobori, Simple methods for estimating the numbers of synonymous and nonsynonymous nucleotide substitutions, Molecular Biology and Evolution **3**, 418 (1986).

[27] R. Zhang and Y. Lin, Deg 5.0, a database of essential genes in both prokaryotes and eukaryotes, Nucleic Acids Research **37**, D455 (2009).

[28] H. Luo, Y. Lin, F. Gao, C.-T. Zhang, and R. Zhang, Deg 10, an update of the database of essential genes that includes both protein-coding genes and noncoding genomic elements, Nucleic Acids Research **42**, D574 (2014).

[29] F. Wright, The "effective number of codons" used in a gene, Gene **87**, 23 (1990).

[30] R. L. Tatusov, D. A. Natale, I. V. Garkavtsev, T. A. Tatusova, U. T. Shankavaram, B. S. Rao, B. Kiryutin, M. Y. Galperin, N. D. Fedorova, and E. V. Koonin, The cog database: New developments in phylogenetic classification of proteins from complete genomes, Nucleic Acids Research **29**, 22 (2001).

[31] M. Y. Galperin, K. S. Makarova, Y. I. Wolf, and E. V. Koonin, Expanded microbial genome coverage and improved protein family annotation in the cog database, Nucleic Acids Research **43**, D261 (2015).

[32] G. Butland, J. M. Peregrin-Alvarez, J. Li, W. Yang, X. Yang, V. Canadien, A. Starostine, D. Richards, B. Beattie, N. Krogan, M. Davey, J. Parkinson, J. Greenblatt, and A. Emili, Interaction network containing conserved and essential protein complexes in escherichia coli, Nature **433**, 531 (2005).

[33] Y. Jin, D. Turaev, T. Weinmaier, T. Rattei, and H. A. Makse, The evolutionary dynamics of protein-protein interaction networks inferred from the reconstruction of ancient networks, PLoS ONE **8**, e58134 (2013).

[34] S. V. Rajagopala, P. Sikorski, A. Kumar, R. Mosca, J. Vlasblom, R. Arnold, J. Franca-Koh, S. B. Pakala, S. Phanse, A. Ceol, R. Häuser, G. Siszler, S. Wuchty, A. Emili, M. Babu, P. Aloy, R. Pieper, and P. Uetz, The binary protein-protein interaction landscape of escherichia coli, Nature Biotechnology **32**, 285 (2014).

[35] M. W. Hahn and A. D. Kern, Comparative genomics of centrality and essentiality in three eukaryotic protein-interaction networks, Molecular Biology and Evolution **22**, 803 (2005).

[36] A. Karimpour-Fard, S. M. Leach, L. E. Hunter, and R. T. Gill, The topology of the bacterial co-conserved protein network and its implications for predicting protein function, BMC Genomics **9**, 313 (2008).

[37] S. Wuchty and P. Uetz, Protein-protein interaction networks of E. coli and S. cerevisiae are similar, Scientific Reports **4**, 7187 (2014).

[38] A. Annibale, A. C. Coolen, and N. Planell-Morell, Protein interaction networks and biology: Towards the connection, arXiv:1501.00662 (2015).

[39] G. D. Bader and C. W. V. Hogue, An automated method for finding molecular complexes in large protein interaction networks, BMC Bioinformatics **4**, 10.1186/1471-2105-4-2 (2003).

[40] B. S. Srinivasan, A. F. Novak, J. A. Flannick, S. Batzoglou, and H. H. McAdams, Integrated protein interaction networks for 11 microbes, in *Research in Computational Molecular Biology: 10th Annual International Conference, RECOMB 2006, Venice, Italy, April 2-5, 2006. Proceedings*, edited by A. Apostolico, C. Guerra, S. Istrail, P. A. Pevzner, and M. Waterman (Springer Berlin Heidelberg, 2006) pp. 1–14.

[41] V. S. Rao, K. Srinivas, G. N. Sujini, and G. N. S. Kumar, Protein-protein interaction detection: methods and analysis, International Journal of Proteomics **2014**, 10.1155/2014/147648 (2014).

[42] H. Jeong, S. P. Mason, A.-L. Barabasi, and Z. N. Oltvai, Lethality and centrality in protein networks, Nature **411**, 41 (2001).

[43] G. E. Fox, Origin and evolution of the ribosome, Cold Spring Harbor Perspectives in Biology **2**, 10.1101/cshperspect.a003483 (2010).

[44] Y.-C. Hwang, C.-C. Lin, J.-Y. Chang, H. Mori, H.-F. Juan, and H.-C. Huang, Predicting essential genes based on network and sequence analysis, Molecular BioSystems **5**, 1672 (2009).

[45] W. Wei, L.-W. Ning, Y.-N. Ye, and F.-B. Guo, Geptop: A gene essentiality prediction tool for sequenced bacterial genomes based on orthology and phylogeny, PLoS ONE **8**, e72343 (2013).

[46] R. Bardini, S. Di Carlo, G. Politano, and A. Benso, Modeling antibiotic resistance in the microbiota using multilevel petri nets, BMC Syst Biol **12**, 108 (2018).

[47] L. Terradot and M.-F. Noirot-Gros, Bacterial protein interaction networks: puzzle stones from solved complex structures add to a clearer picture, Integrative Biology **3**, 645 (2011).

[48] R. Zoraghi and N. E. Reiner, Protein interaction networks as starting points to identify novel antimicrobial drug targets, Curr Opin Microbiol **16**, 566 (2013).

[49] T. Sevimoglu and K. Y. Arga, The role of protein interaction networks in systems biomedicine, Computational and Structural Biotechnology Journal **11**, 22 (2014).

[50] S. Boccaletti, G. Bianconi, R. Criado, C. del Genio, J. G.-G. nes, M. Romance, I. S. na Nadal, Z. Wang, and M. Zanin, The structure and dynamics of multilayer networks, Physics Reports **544**, 1 (2014).

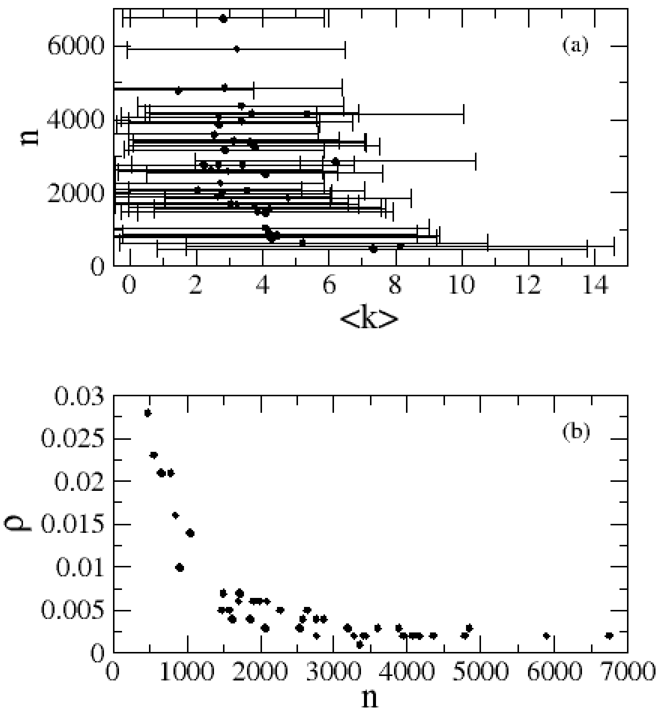

FIG. S7. Relation between genome size n and average degree $\langle k \rangle \pm \sigma_k$ (upper panel) and density ρ (bottom panel) of the corresponding PPI network for the set of bacteria collected in Table I.The density of a network is the ratio between the actual number of links and the number of links in the fully connected case, namely $\frac{1}{2}n(n-1)$.

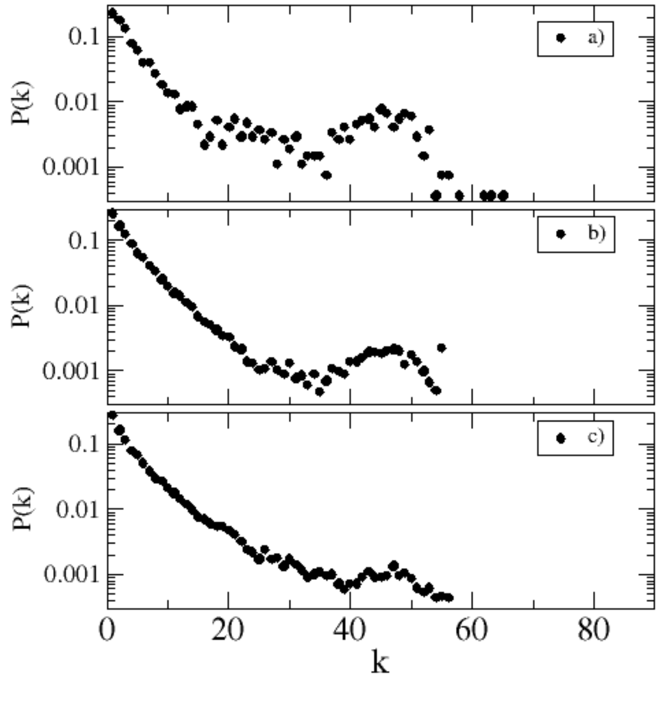

FIG. S8. Distributions of PPI degree $P(k)$ averaged over the PPI networks of the three groups of bacteria in Table I, subdivided according to the number n of their genes: a) $n < 1000$, b) $1000 < n < 3000$ and c) $n > 3000$. Clearly, the "bump" at $k > 40$ in Figure 1 is a feature that is characteristic of small genomes (groups a and b), mostly constituted by essential genes. In the genomes of group c the interactions that constitute the bump are diluted among the other interactions due to non essential genes. This dilution effect can be seen also in the subsequent figures S10, S11, S12, S13

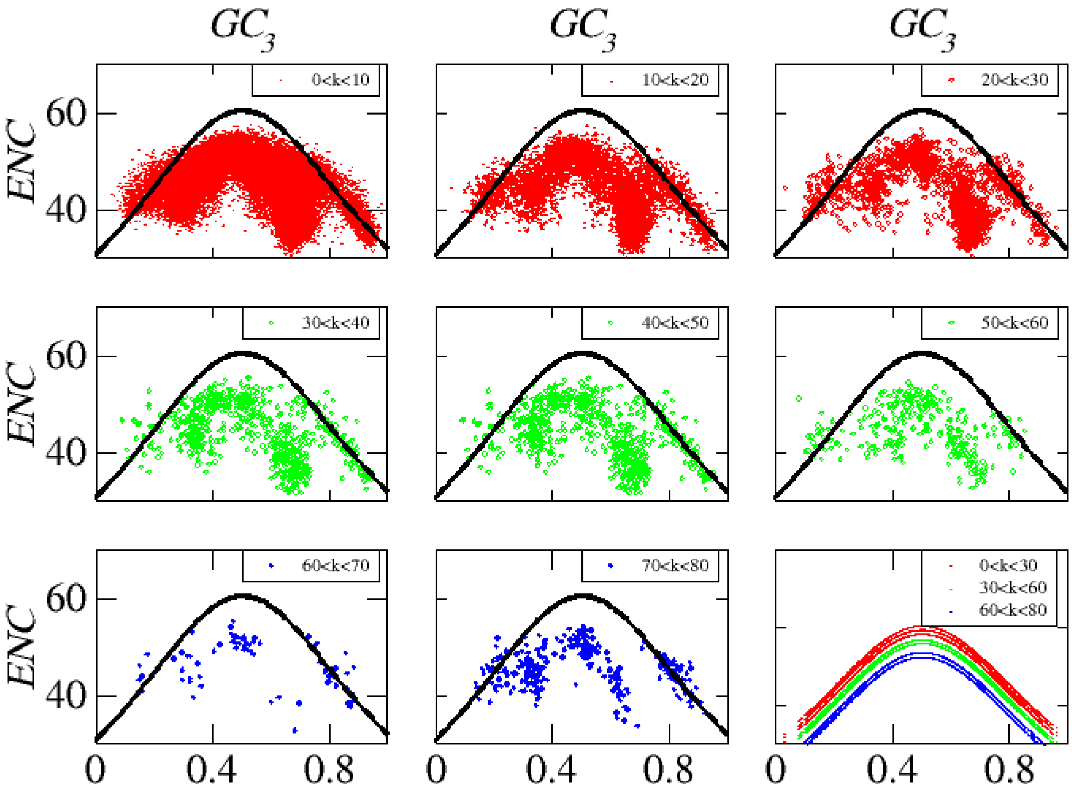

FIG. S9. ENC plots for three groups of genes corresponding to proteins with different degree connectivities k. In each panel the solid black lines are plots of Wright's theoretical curve (equation (2)) which correlates effective number of codons with GC_3 in the case of pure mutational bias (no selective pressure). Coherently with Figures 3 and 4, the case of low connectivities are shown in red, intermediate in green and high connectivities in blue. In the bottom-right panel dashed non-linear fits of Wright's theoretical shapes to the experimental data. For the sake of completeness the best fit parameters are reported in the following Table VI.

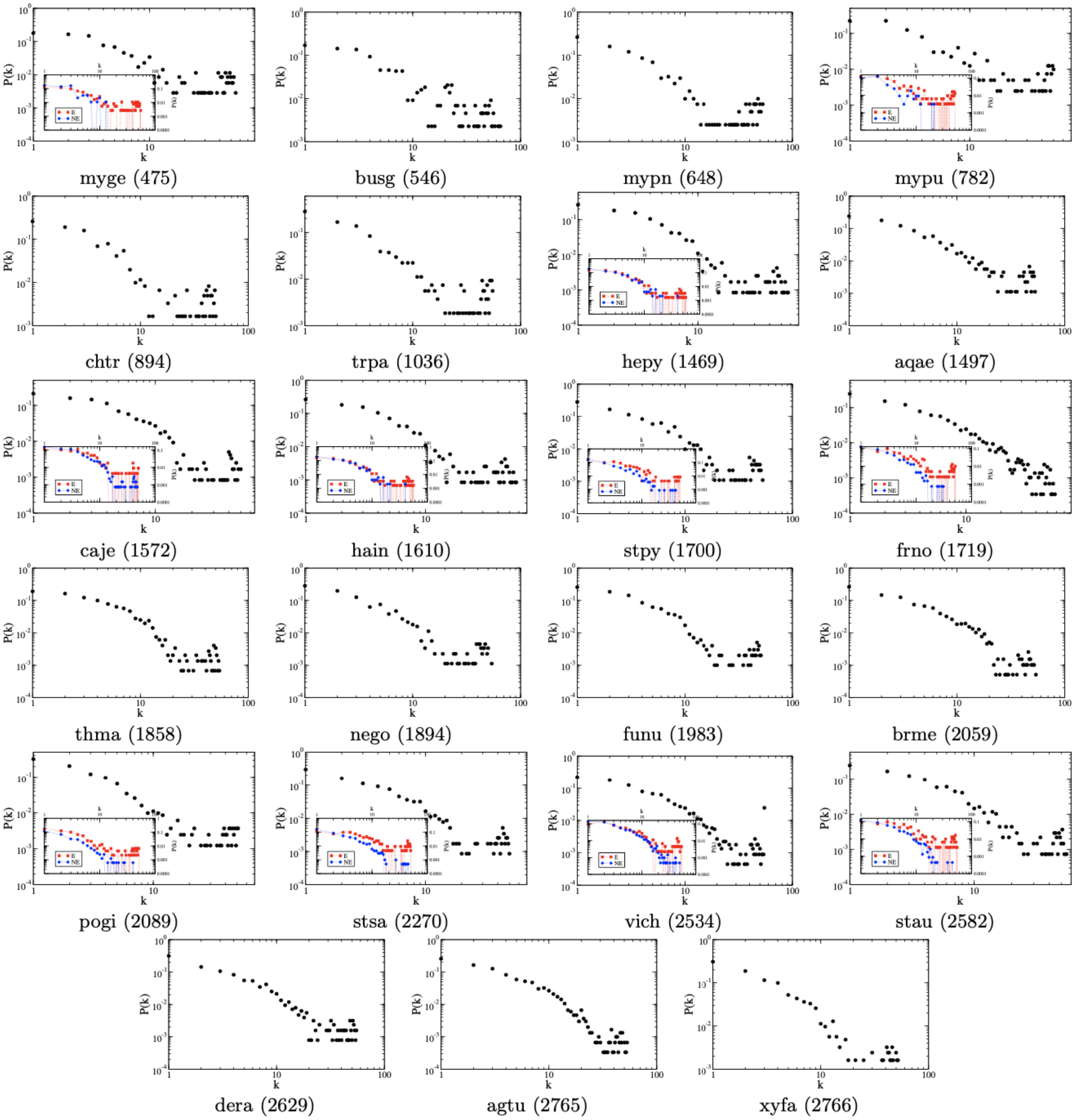

myge (475) busg (546) mypn (648) mypu (782)

chtr (894) trpa (1036) hepy (1469) aqae (1497)

caje (1572) hain (1610) stpy (1700) frno (1719)

thma (1858) nego (1894) funu (1983) brme (2059)

pogi (2089) stsa (2270) vich (2534) stau (2582)

dera (2629) agtu (2765) xyfa (2766)

FIG. S10. Degree distributions $P(k)$ (part 1, small genomes) of some of the bacteria collected in Table I, sorted by the increasing size n of their genomes. For DEG-annotated genomes, the inset shows the contribution of essential (red) and nonessential (blue) genes. Note, for $k > 40$, in many cases the presence of a structure, particularly evident in the $P(k)$ of the essential genes, that likely contributes to the bump in Figure 1.

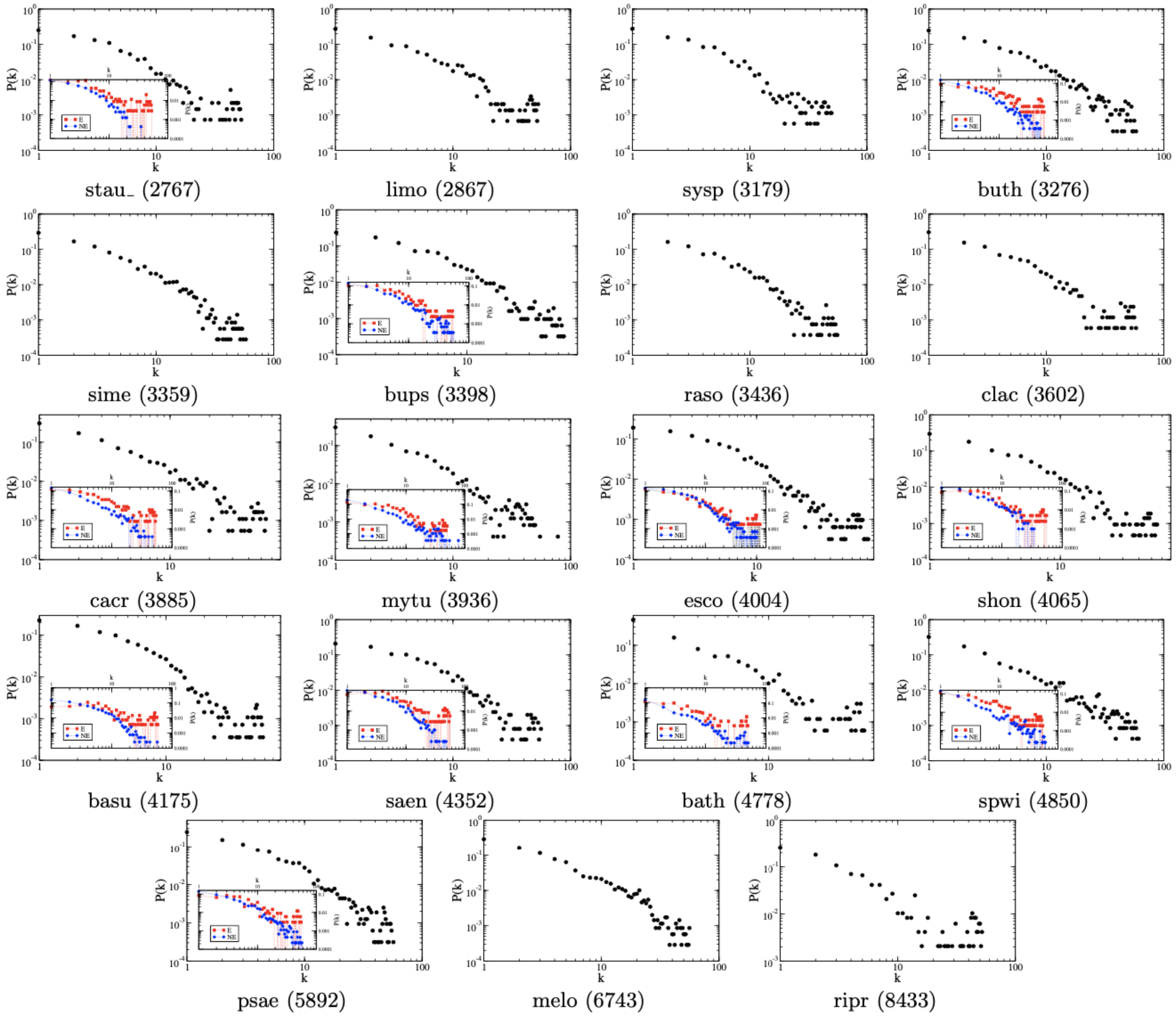

stau_ (2767)

limo (2867)

sysp (3179)

buth (3276)

sime (3359)

bups (3398)

raso (3436)

clac (3602)

cacr (3885)

mytu (3936)

esco (4004)

shon (4065)

basu (4175)

saen (4352)

bath (4778)

spwi (4850)

psae (5892)

melo (6743)

ripr (8433)

FIG. S11. Degree distributions $P(k)$ (part 2, big genomes) of the PPI networks for some of the bacteria collected in Table I, ordered by the increasing size n of their genomes. For DEG-annotated genomes, the inset shows the contribution of essential (red) and nonessential (blue) genes. Note that, in most cases, in the region $k > 40$, the signature of the bump is blurred, hidden behind a general power law trend, likely due to the contribution of the interactions of non essential genes, as shown in the subsequent figures: S12 and S13.

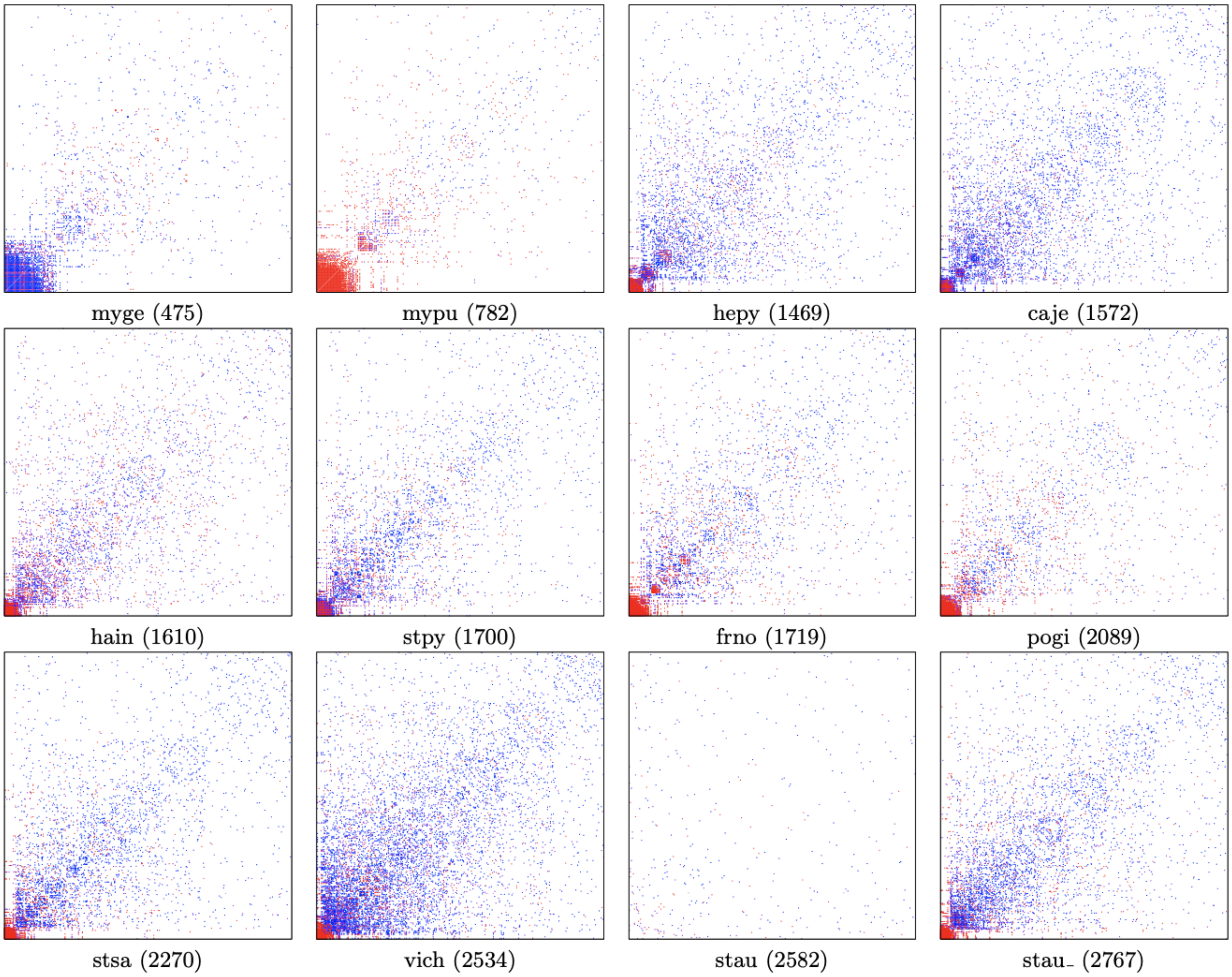

myge (475)

mypu (782)

hepy (1469)

caje (1572)

hain (1610)

stpy (1700)

frno (1719)

pogi (2089)

stsa (2270)

vich (2534)

stau (2582)

stau$_{-}$ (2767)

FIG. S12. Adjacency matrices (part 1, small genomes) of PPI networks for the DEG-annotated bacterial species collected in Table I. From top left the matrices are sorted according to the increasing size of the bacterial genomes. In each matrix, genes are ordered according to the decreasing degree of the corresponding protein in the network, from left to right (horizontal axis) and from bottom to top (vertical axis). Links between essential genes are plotted as a red dot, those between nonessential (and non-annotated) genes with blue dots, and those between essential and nonessential (plus non-annotated) genes with a violet dot. The red spot in the lower left sector of each matrix corresonds to the core of genes of the highly connected proteins of the almost-invariant structure of ribosomal hubs. Overall, in the case of small genomes it is evident how the red subnets of the essential genes dominate the matrices. In bigger genomes, as also shown in the next figure, the blue non-essential with non-essential gene interactions and the violet cross-interactions tend to superpose to the core of the essential genes. It is worth noting that it could be reasonable to evaluate how much a PPI is relatively covered, in each species by the relative occurrence of blue and violet dots normalized to the maximal number of links in the network

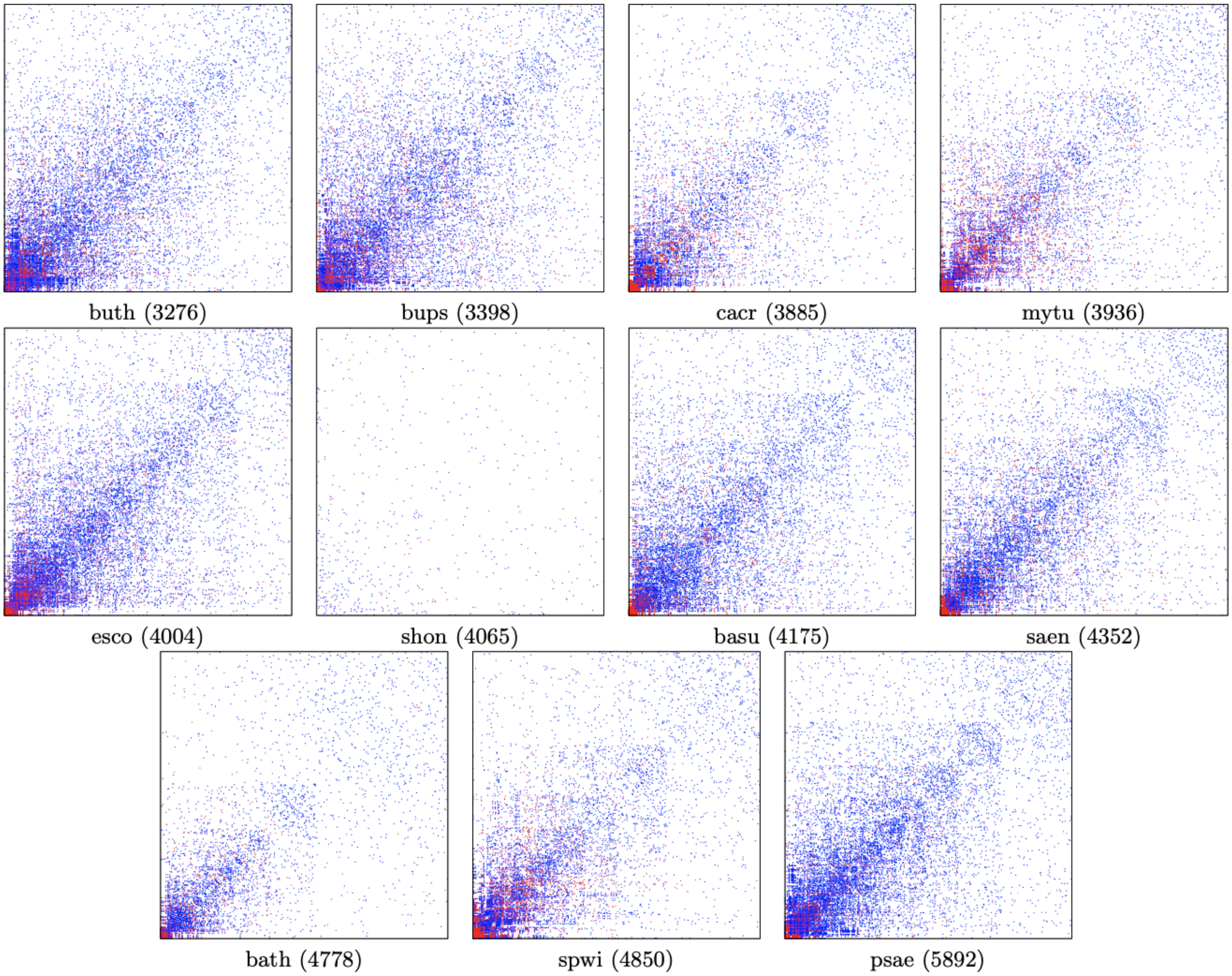

buth (3276)

bups (3398)

cacr (3885)

mytu (3936)

esco (4004)

shon (4065)

basu (4175)

saen (4352)

bath (4778)

spwi (4850)

psae (5892)

FIG. S13. Adjacency matrices (part 2, big genomes) of PPI networks for the DEG-annotated bacterial species collected in Table I. From top left the matrices are sorted according to the increasing size of the bacterial genomes. In each matrix, genes are ordered according to the decreasing degree of the corresponding protein in the network, from left to right (horizontal axis) and from bottom to top (vertical axis). Links between essential genes are plotted as a red dot, those between nonessential (and non-annotated) genes with blue dots, and those between essential and nonessential (plus non-annotated) genes with a violet dot. Also looking at these graphs one would be tempted to possibly associate the relative presence of blue interactions to the extent the interactome is known and annotated

Organisms	**Abbr.**	**Class**	**RefSeq**	**STRING**	**n**
Mycoplasma genitalium G37	myge	10	NC_000908	243273	475
Buchnera aphidicola Sg uid57913	busg	2	NC_004061	198804	546
Mycoplasma pneumoniae M129	mypn	10	NC_000912.1	272634	648
Mycoplasma pulmonis UAB CTIP	mypu	10	NC_002771	272635	782
Chlamydia trachomatis D/UW-3/CX	chtr	14	NC_000117.1	272561	894
Treponema pallidum Nichols	trpa	11	NC_000919.1	243276	1036
Helicobacter pylori 26695	hepy	4	NC_000915	85962	1469
Aquifex aeolicus VF5	aqae	12	NC _000918	224324	1497
Campylobacter jejuni	caje	4	NC_002163	192222	1572
Haemophilus influenzae Rd KW20	hain	3	NC_000907.1	71421	1610
Streptococcus pyogenes NZ131	stpy	6	NC_011375	471876	1700
Francisella novicida U112	frno	3	NC_008601	401614	1719
Thermotoga maritima MSB8	thma	16	NC_000853.1	243274	1858
Neisseria gonorrhoeae FA 1090 uid57611	nego	2	NC_002946	242231	1894
Fusobacterium nucleatum ATCC 25586	funu	15	NC_003454.1	190304	1983
Brucella melitensis bv. 1 str. 16M	brme	1	NC_003317.1	224914	2059
Porphyromonas gingivalis ATCC 33277	pogi	7	NC_010729	431947	2089
Streptococcus sanguinis	stsa	6	NC_009009	388919	2270
Vibrio cholerae N16961	vich	3	NC_002505	243277	2534
Staphylococcus aureus N315	stau	6	NC_002745.2	158879	2582
Deinococcus radiodurans R1	dera	9	NC_001263.1	243230	2629
Agrobacterium tumefaciens (fabrum)	agtu	1	NC_003062	176299	2765
Xylella fastidiosa 9a5c	xyfa	3	NC_002488	160492	2766
Staphylococcus aureus NCTC 8325	stau_	6	NC_007795	93061	2767
Listeria monocytogenes EGD-e	limo	6	NC_003210.1	169963	2867
Synechocystis sp. PCC 6803	sysp	13	NC_000911.1	1148	3179
Burkholderia thailandensis E264	buth	2	NC_007651	271848	3276
Sinorhizobium meliloti 1021	sime	1	NC_003047.1	266834	3359
Burkholderia pseudomallei K96243	bups	3	NC_006350	272560	3398
Ralstonia solanacearum GMI1000	raso	2	NC_003295.1	267608	3436
Clostridium acetobutylicum ATCC 824	clac	8	NC_003030.1	272562	3602
Caulobacter crescentus	cacr	1	NC_011916	565050	3885
Mycobacterium tuberculosis H37Rv	mytu	5	NC_000962.3	83332	3936
Escherichia Coli K-12 MG1655	esco	3	NC_000913.3	511145	4004
Shewanella oneidensis MR-1	shon	3	NC_004347	211586	4065
Bacillus subtilis 168	basu	6	NC_000964	224308	4175
Salmonella enterica serovar Typhi	saen	3	NC_004631	209261	4352
Bacteroides thetaiotaomicron VPI-5482	bath	7	NC_004663	226186	4778
Sphingomonas wittichii RW1	spwi	1	NC_009511	392499	4850
Pseudomonas aeruginosa UCBPP-PA14	psae	3	NC_008463	208963	5892
Mesorhizobium loti MAFF303099	melo	1	NC_002678.2	266835	6743
Rickettsia prowazekii str. Madrid E	ripr	1	NC_000963.1	272947	8433

TABLE I. Summary of the selected bacterial dataset. Organism name, abbreviation, class, RefSeq, STRING code, size of genome (number of genes n). Genomes annotated in the Database of Essential Genes (DEG) are highlighted with bold fonts. Classes are:Alphaproteobacteria(1), Betaproteobacteria(2), Gammaproteobacteria(3), Epsilonproteobacteria(4), Actinobacteria(5), Bacilli(6), Bacteroidetes(7), Clostridia(8), Deinococci(9), Mollicutes(10), Spirochaetales(11), Aquificae(12), Cyanobacteria(13), Chlamydiae(14), Fusobacteria(15), Thermotoga(16).

COG ID	Functional classification
	INFORMATION STORAGE AND PROCESSING
J	Translation, ribosomal structure and biogenesis
K	Transcription
L	Replication, recombination and repair
	CELLULAR PROCESSES AND SIGNALING
D	Cell cycle control, cell division, chromosome partitioning
T	Signal transduction mechanisms
M	Cell wall/membrane/envelope biogenesis
N	Cell motility
O	Post-translational modification, protein turnover, chaperones
	METABOLISM
C	Energy production and conversion
G	Carbohydrate transport and metabolism
E	Amino acid transport and metabolism
F	Nucleotide transport and metabolism
H	Coenzyme transport and metabolism
I	Lipid transport and metabolism
P	Inorganic ion transport and metabolism

TABLE II. Functional classification of COG clusters.

Organisms	r_{ee}	$r_{\bar{e}\bar{e}}$	$r_{e\bar{e}}$
basu	44.46	0.80	0.11
bath	20.07	0.76	0.25
bups	6.21	0.83	0.27
buth	18.69	0.70	0.22
cacr	18.40	0.70	0.15
caje	3.65	0.82	0.32
esco	2.91	0.88	0.31
frno	9.84	0.52	0.18
hain	1.65	1.15	0.27
hepy	2.91	0.78	0.38
myge	1.42	0.29	0.08
mypu	3.42	0.22	0.12
mytu	8.09	0.78	0.23
pogi	11.03	0.41	0.21
psae	9.85	0.92	0.16
saen	28.80	0.81	0.12
shon	6.50	0.64	0.16
spwi	15.47	0.74	0.22
stau	23.05	0.58	0.23
stau_	21.89	0.64	0.16
stpy	9.30	0.73	0.23
stsa	30.65	0.61	0.22
vich	8.37	0.81	0.19

TABLE III. Relative density values r for PPI subnetworks between essential genes (r_{ee}), between nonessential genes ($r_{\bar{e}\bar{e}}$) and between essential and nonessential genes ($r_{e\bar{e}}$), for each DEG-annotated bacterial genome.

k	**COG**	**Gene**	**Protein**
57	1250I	paaH	3-hydroxyadipyl-CoA dehydrogenase, NADdependent
	0365I	acs	acetyl-CoA synthetase
58	0222J	rplL	50S ribosomal subunit protein L7/L12
	0335J	rplS	50S ribosomal subunit protein L19
	0267J	rpmG	50S ribosomal subunit protein L33
	0365I	acs	acetyl-CoA synthetase
59	0183I	paaJ	3-oxoadipyl-CoA3-oxo-5,6-dehydrosuberyl-CoA thiolase
	1960I	ydiO	putative acyl-CoA dehydrogenase
	0183I	atoB	acetyl-CoA acetyltransferase
60	0197J	rplP	50S ribosomal subunit protein L16
	0088J	rplD	50S ribosomal subunit protein L4
	0197J	rplP	50S ribosomal subunit protein L16
	0087J	rplC	50S ribosomal subunit protein L3
	1960I	aidB	putative acyl-CoA dehydrogenase
61	0085K	rpoB	RNA polymerase, beta subunit
	0202K	rpoA	RNA polymerase, alpha subunit
62	0087J	rplC	50S ribosomal subunit protein L3
	0052J	rpsB	30S ribosomal subunit protein S2
	2965L	PriB	ribosomal replication protein

TABLE IV. Specifics of the hub proteins that populate the few bins of connectivity around $k = 60$ in Figure 5.

COG	**Genes name**	**<k >**
COG0097J	50S ribosomal protein L6	60.24
COG0087J	50S ribosomal protein L3	60.19
COG0197J	50S ribosomal protein L16	60.19
COG0090J	50S ribosomal protein L2	60.14
COG0080J	50S ribosomal protein L11	60.12
COG0088J	50S ribosomal protein L4	60.12
COG0081J	50S ribosomal protein L1	58.19
COG0089J	50S ribosomal protein L23	57.88
COG0102J	50S ribosomal protein L13	57.45
COG0094J	50S ribosomal protein L5	57.21
COG0092J	30S ribosomal protein S3	57.12
COG0098J	30s ribosomal protein S5	57.10
COG0093J	50S ribosomal protein L14	57.00
COG0091J	50S ribosomal protein L22	56.24
COG0049J	30S ribosomal protein S7	55.31
COG0051J	30S ribosomal protein S10	55.24
COG0200J	50S ribosomal protein L15	55.12
COG0256J	50S ribosomal protein L18	54.86
COG0203J	50S ribosomal protein L17	54.43
COG0244J	50S ribosomal Protein L10	54.19
COG0100J	30S ribosomal protein S11	53.76
COG0522J	30S ribosomal protein S4	53.43
COG0096J	30S ribosomal protein S8	53.10
COG0099J	30S ribosomal protein S13	52.88
COG0048J	30S ribosomal protein S12	52.14
COG0198J	50S ribosomal protein L24	50.83
COG0185J	30S ribosomal protein S19	50.52
COG0199J	30S ribosomal protein S14	50.45
COG0103J	30S ribosomal protein S9	49.45
COG0480J	tetracycline resistance protein. tetM	47.90
COG0052J	30S ribosomal protein S2	47.69
COG0184J	30S ribosomal protein S15	45.95
COG0186J	30S ribosomal protein S17	44.60
COG0255J	50S ribosomal protein L29	43.95
COG0222J	50S ribosomal protein L7/L12	42.43
COG1841J	50S ribosomal protein L30	40.71

TABLE V. Genes belonging to COG J with average degree bigger than 40 (see Figure 6). All these genes are conserved, common to all species (ERI=1), and drive the transition shown in Figure 5

.

k	**a**	**b**	**c**	**d**	R^2
$[0-10]$	40,561	-10,338	5,555	1,052	0,617
$[10-20]$	23,774	3,890	8,583	0,626	0,590
$[20-30]$	20,280	8,287	8,276	0,507	0,540
$[30-40]$	18,296	10,685	8,334	0,190	0,790
$[40-50]$	18,548	10,372	8,326	0,495	0,589
$[50-60]$	25,868	2,508	8,038	0,650	0,758
$[60-70]$	29,344	-0,756	10,224	0,977	0,870
$[70-80]$	30,507	3,438	6,990	0,811	0,874

TABLE VI. Best fit values of the parameters in equation (2) and correlation coefficients for different connectivity data, shown in figure S9.